

Transonic flow past a Whitcomb airfoil with a deflected aileron

Alexander Kuzmin*

St. Petersburg State University, St. Petersburg, Russia

Abstract

The sensitivity of transonic flow past a Whitcomb airfoil to deflections of an aileron is studied at free-stream Mach numbers from 0.81 to 0.86 and vanishing or negative angles of attack. Solutions of the Reynolds-averaged Navier-Stokes equations are obtained with a finite-volume solver using the $k-\omega$ SST turbulence model. The numerical study demonstrates the existence of narrow bands of the Mach number and aileron deflection angles that admit abrupt changes of the lift coefficient at small perturbations. In addition, computations reveal free-stream conditions in which the lift coefficient is independent of aileron deflections of up to 5 degrees. The anomalous behavior of the lift is explained by interplay of local supersonic regions on the airfoil. Both stationary and impulse changes of the aileron position are considered.

Key words: Local supersonic regions, Aileron deflection, Instability, Lift coefficient

1. Introduction

The correct prediction of the effectiveness of wing control surfaces (ailerons and spoilers) is of major importance in the process of aircraft design. The development of numerical methods enables accurate simulation of transonic flow over control surfaces with fixed deflection angles [1, 2]. A number of studies examined transonic flow over time-dependent flaps, as well as aeroelastic behavior of airfoils and wings [3–5]. However, the flow sensitivity to small perturbations in various bands of the angle of attack and Mach number has not been subject to detailed analysis.

The upward deployment of an aileron or spoiler flattens the profile in the vicinity of the aileron-airfoil juncture or even makes it locally concave. In the 2000s, a number of numerical studies demonstrated a high sensitivity of transonic flow to variations of free-stream parameters when the airfoil comprises a flat or nearly flat arc. The sensitivity is caused by the interaction of two supersonic regions that arise and expand on the arc as the free-stream Mach number increases. The expansion followed by a coalescence of the supersonic regions crucially changes pressure distributions and aerodynamic loads on the airfoil. This phenomenon

was scrutinized for a number of symmetric profiles [6–7], as well as for the asymmetric J-78 airfoil whose upper surface is nearly flat in the midchord region [6, 8]. Also the instability of closely spaced supersonic regions was examined for a Whitcomb airfoil with a deflected aileron at the Reynolds number $Re=5.6 \times 10^6$ [9].

In this paper, we study transonic flow past a Whitcomb airfoil with aileron deflections at the vanishing or negative angles of attack, which are typical for a descending flight of civil and transport aircraft, at $Re=1.4 \times 10^7$. The emphasis is laid on the flow physics and free-stream conditions that admit anomalous behavior of the lift coefficient.

2. Problem formulation

We consider a fully turbulent 2D flow past an airfoil given by the expressions

$$y=y_{\text{whit}}(x) \quad \text{at } 0 \leq x \leq 0.7, \quad (1a)$$

$$y=y_{\text{whit}}(x) + (x-0.7) \tan \theta \quad \text{at } 0.7 \leq x \leq 1 \quad (1b)$$

where x and y are non-dimensional Cartesian coordinates,

This is an Open Access article distributed under the terms of the Creative Commons Attribution Non-Commercial License (<http://creativecommons.org/licenses/by-nc/3.0/>) which permits unrestricted non-commercial use, distribution, and reproduction in any medium, provided the original work is properly cited.

© * Dr.Sc., Head researcher, Corresponding author : alexander.kuzmin@pobox.spbu.ru

and $y_{\text{whit}}(x)$ refers to the Whitcomb integral supercritical airfoil [10]. The last term in (1b) shifts the rear part of the airfoil upward, simulating an aileron rotation at a small angle θ , as illustrated in Fig. 1. The airfoil is placed at the center of a lens-type computational domain, bounded by two circular arcs, Γ_1 : $x(y) = 105 - (145^2 - y^2)^{1/2}$ and Γ_2 : $x(y) = -105 + (145^2 - y^2)^{1/2}$, $-100 \leq y \leq 100$. The width and height of the domain are 80 and 200, respectively. We set the length L_{chord} of the airfoil chord to 2.5 m.

On the inflow part Γ_1 of the boundary, we prescribe stationary values of the angle of attack α , free-stream Mach number $M_\infty < 1$, and static temperature $T_\infty = 223.15$ K. On the outflow boundary Γ_2 , we impose the static pressure $p_\infty = 26,434$ N/m². The above values of T_∞ and p_∞ are respective to the standard atmosphere at a height of 10 km. The no-slip condition and vanishing flux of heat are used on the airfoil. The air is assumed to be a perfect gas whose specific heat at constant pressure is 1004.4 J/(kg K) and the ratio of specific heats is 1.4. We adopt the value of 28.96 kg/kmol for the molar mass, and use the Sutherland formula for the molecular dynamic viscosity. Initial data are parameters of the uniform free-stream, in which the turbulence level was set to 0.2%.

3. A numerical method

Solutions of the RANS equations were obtained with the ANSYS 13 CFX finite-volume solver based on a high-resolution discretization scheme for convective terms [11]. We employed an implicit second-order accurate backward Euler scheme for the time-stepping. Computations were performed on hybrid unstructured meshes of about 4×10^5 cells, which were clustered in the boundary layer, in the

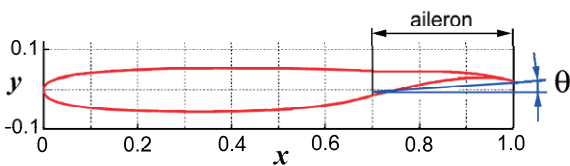


Fig. 1. Sketch of the Whitcomb airfoil with an aileron deflection at a positive angle θ .

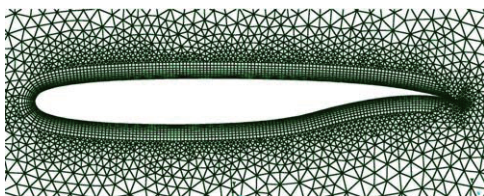


Fig. 2. Sketch of the computational mesh in a vicinity of the airfoil.

wake, and in the vicinities of the shock waves. The non-dimensional thickness y^+ of the first mesh layer on the airfoil was less than 1 (see Fig. 2). We used the standard $k-\omega$ Shear Stress Transport turbulence model, which reasonably predicts aerodynamic flows with boundary layer separations from smooth surfaces [12].

The solver was verified by computation of solutions for a few benchmark problems and comparison with experimental and numerical data available in the literature. Figure 3 shows good agreement of the lift coefficient $C_L(\alpha)$ calculated for a RAE 2822 airfoil at $-1 \leq \alpha$, $\text{deg} \leq 3$ with results obtained in [13-17]. Also the solver was used for the simulation of an oscillatory transonic flow past a 18% thick circular-arc airfoil at zero angle of attack and $\text{Re} = 1.1 \times 10^7$. The amplitude of lift coefficient oscillations at $M_\infty = 0.75$ was 0.35. This agrees well with the value of 0.37 obtained numerically in [18] using the Spalart-Allmaras and Baldwin-Lomax turbulence models.

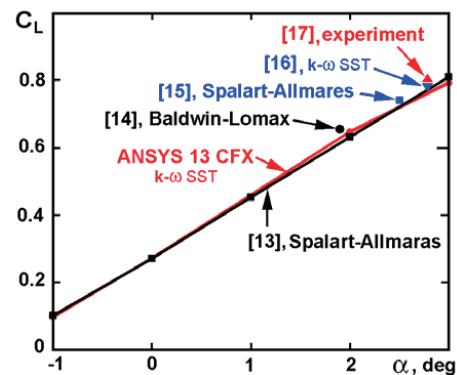


Fig. 3. Lift coefficient versus the angle of attack for a test case of transonic flow over the RAE 2822 airfoil at $M_\infty = 0.73$, $\text{Re} = 6.5 \times 10^6$. The references to numerical studies are accompanied by the information on turbulence models used.

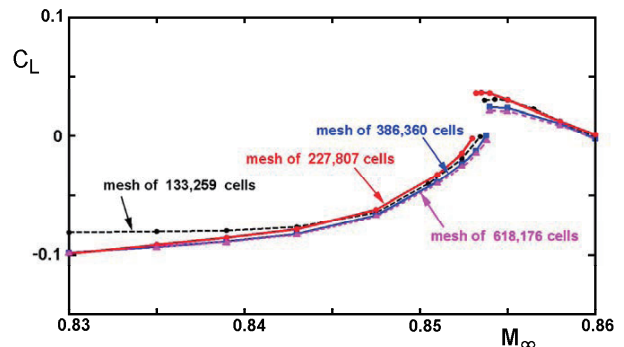


Fig. 4. Convergence of the lift coefficient with mesh refinement for airfoil (1) at the aileron deflection angle $\theta = 4$ deg, angle of attack $\alpha = -0.8$ deg, and Reynolds number $\text{Re} \approx 1.4 \times 10^7$.

4. Results and discussion

In the case of stationary boundary conditions, steady-state solutions were obtained by the global time-stepping in 2 to 6 seconds. The solutions yield a flow field, as well as aerodynamic forces on the airfoil. This makes it possible to calculate the lift coefficient $C_L = 2F / (\rho_\infty U_\infty^2 S)$, where F is the normal force, U_∞ is the free-stream velocity module, and S is the wing area in planform. For the simulation of 2D flow we used 3D meshes with one cell of length $L_z = 0.01$ m in the z -direction, so that $S = L_{\text{chord}} \times L_z = 0.025$ m². Figure 4 displays plots of the lift coefficient versus M_∞ calculated on three different meshes at the angle of attack $\alpha = -0.8$ deg and the aileron deflection angle $\theta = 4$ deg. Evidently, the mesh of

386,360 cells provides a good accuracy of the solution.

Figure 5 illustrates the obtained dependence of the lift coefficient C_L on two parameters, M_∞ and θ , for airfoil (1) at the angles of attack $\alpha = 0$ and $\alpha = -0.8$ deg. As seen from Fig. 5a, if $\alpha = 0$ and $M_\infty < 0.838$, then a deflection of the aileron from zero to three degrees entails a considerable fall of the lift coefficient. This is caused by a rapid shrinking of the supersonic region on the upper surface and expansion of the supersonic region on the lower surface of the airfoil. If $\alpha = -0.8$ deg, then abrupt changes of C_L take place at larger values of M_∞ and $3.5 < \theta < 5$, so that the surface $C_L(M_\infty, \theta)$ comprises a slit at $0.846 < M_\infty \leq 0.86$ (see Fig. 5b).

At the same time Figs. 5a and 5b show that, when $M_\infty > 0.855$, the lift coefficient is independent of aileron deflections up to 5 and 4 degrees, respectively. This can be

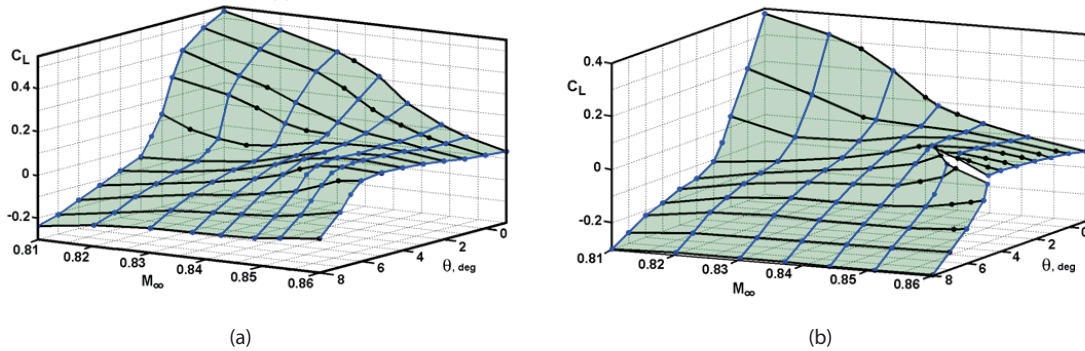


Fig. 5. Lift coefficient as a function of the aileron deflection angle θ and Mach number M_∞ for transonic flow past airfoil (1) at $Re \approx 1.4 \times 10^7$: (a) $\alpha = 0$, (b) $\alpha = -0.8$ deg.

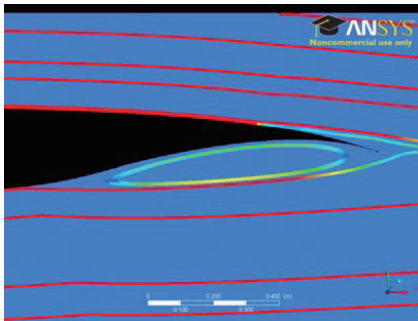


Fig. 6. Streamlines in a vicinity of the trailing edge at $M_\infty = 0.86$, $\alpha = -0.8$ deg, $\theta = 0$.

explained again by the interplay of local supersonic regions. Indeed, Figure 6 shows that at $\theta = 0$ the airfoil's trailing edge resides in a stagnation zone above the streamline separated from the lower surface of the airfoil. That is why moderate upward deflections of the aileron do not influence the flow field. With increasing aileron deflection angle from 0 to 4 deg, the supersonic regions slightly expand on both surfaces (see Fig. 7), that is why the lift coefficient persists. If the angle θ further increases, then the supersonic region on the upper surface shrinks, while that on the lower surface expands. As a consequence, the static pressure drops on the lower surface, and the lift coefficient drops.

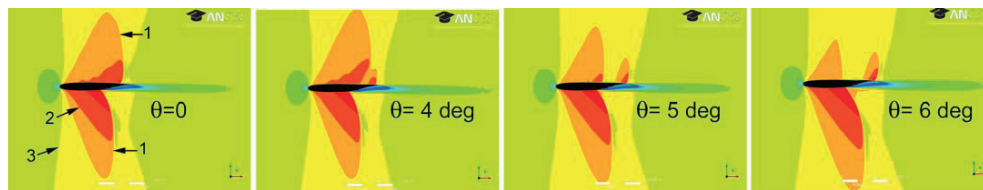


Fig. 7. Evolution of the local supersonic regions in transonic flow past airfoil (1) at the increasing angle θ of the aileron deflection and $M_\infty = 0.86$, $\alpha = -0.8$ deg, $Re = 1.4 \times 10^7$. Mach number contours: 1 – $M = 1.0$, 2 – $M = 1.125$, 3 – $M = 0.875$.

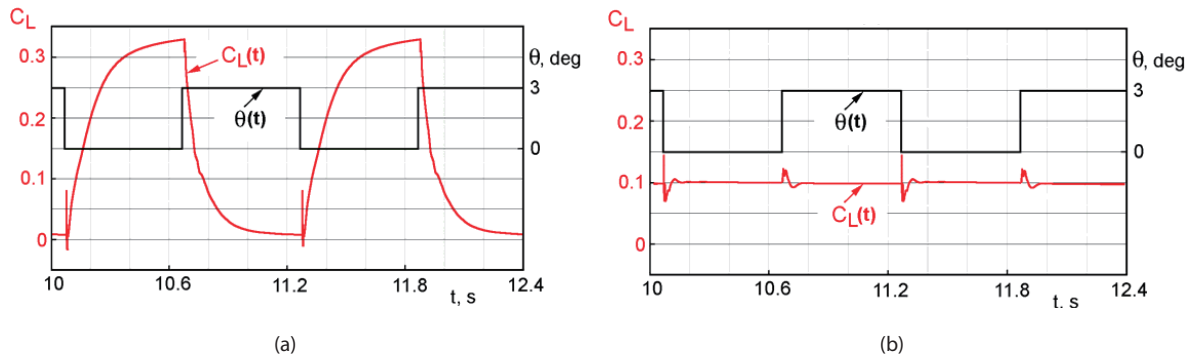


Fig. 8. Lift coefficient as a function of time for airfoil (1) at $\alpha=0$, $Re \approx 1.4 \times 10^7$, and periodic impulse changes of the deflection angle θ : (a) $M_\infty=0.83$, (b) $M_\infty=0.85$.

Also we considered a time-dependent aileron deflection $\theta(t)$ that switches between 0 and 3 deg every 0.6 s, with a period of 1.2 s. Figure 8a shows a calculated dependence of the lift coefficient on time at $M_\infty=0.83$ and $\alpha=0$. An increase of M_∞ to 0.85 results in a crucial reduction of the amplitude of lift coefficient oscillations (see Fig. 8b) in accordance with Fig. 5a exhibiting C_L versus stationary variations of θ .

5. Conclusions

For the airfoil at hand, there exist adverse free-stream conditions that admit abrupt changes of the lift coefficient at small variations of the aileron deflection angle. Conversely, there exist conditions in which a response of the lift coefficient to aileron deflections is anomalously weak, so that the aileron fails to control the lift. Both anomalous phenomena are caused by the interplay of local supersonic regions on the airfoil.

Acknowledgement

This research was performed using computational resources provided by the Computational Center of St. Petersburg State University (<http://cc.spbu.ru>). The work was supported by the Russian Foundation for Basic Research under grant no. 13-08-00288.

References

- [1] Henry, M.M., *Two-dimensional shock sensitivity analysis for transonic airfoils with leading-edge and trailing-edge device deflections*, Master's thesis, Virginia Polytechnic Institute, Blacksburg, Virginia, 2001.
- [2] Méheut, M., Atinault, O., and Hantrais-Gervois, J.-L., "elsA and TAU assessment for wing control surfaces", *Research Report*, TP 2011-102, ONERA, Toulouse, France, 2011.
- [3] Dimitrov, D., "Unsteady aerodynamics of wings with an oscillating flap in transonic flow", *8th PEGASUS-AIAA Student Conference*, Poitiers, Frankreich, 2012.
- [4] Reimer, L., and Heinrich, R., "Modeling of movable control surfaces and atmospheric effects", *Notes on numerical fluid mechanics and multidisciplinary design*, Vol. 123, 2013, pp. 183-206.
- [5] Blanc, F., Roux, F.-X., and Jouhaud, J.-Ch., "Numerical methods for control surfaces aerodynamics with flexibility effects", *International Forum on Aeroelasticity and Structural Dynamics 2009*, CERFACS, Toulouse, France, 2009, pp. 1-15, URL : http://www.cerfacs.fr/~cfdbib/repository/TR_CFD_09_54.pdf
- [6] Kuzmin, A., "Non-unique transonic flows over airfoils", *Computers and Fluids*, Vol. 63, 2012, pp. 1-8.
- [7] Jameson, A., Vassberg, J.C., and Ou, K., "Further studies of airfoils supporting non-unique solutions in transonic flow", *AIAA Journal*, Vol. 50, No. 12, 2012, pp. 2865-2881.
- [8] Kuzmin A., Bifurcations of transonic flow past flattened airfoils. E-print, Centre pour la Communication Scientifique Directe, 2009, pp. 1-11, URL : <http://hal.archives-ouvertes.fr/hal-00433168>
- [9] Kuzmin, A., and Ryabinin, A., "Airfoils admitting anomalous behavior of lift coefficient in descending transonic flight", *The Seventh Intern. Conference on Comput. Fluid Dynamics*, Hawaii, USA, 2012, pp. 1-7, URL : <http://www.iccfd.org/iccfd7>
- [10] Airfoil Coordinate Database. UIUC Applied Aerodynamics Group, 1995-2013. URL : <https://aerodynamics.lr.tudelft.nl/cgi-bin/afCDb/>
- [11] Barth, T.J., and Jespersen, D.C., "The design and application of upwind schemes on unstructured meshes", *AIAA Paper*, 89-0366, 1989, pp. 1-12.
- [12] Menter, F.R., "Review of the Shear-Stress Transport

turbulence model experience from an industrial perspective”, *Intern. J. Comput. Fluid Dynamics*, Vol. 23, Issue 4, 2009, pp. 305-316.

[13] Barrett, Th.R., *Aerodynamic design optimization using flow feature parametrization*, PhD thesis, University of Southampton, School of Engineering Sciences, Southampton, UK, 2007.

[14] Hazra, S.B., “Large-scale PDE-constrained optimization in applications”, *Lecture Notes in Applied and Computational Mechanics*, Vol. 49, Springer, 2010.

[15] Yang, J.Y., Hsieh, T.-J., and Huang, J.C., “Implicit implementation of variant WENO schemes for compressible flow computations”, *Computational Fluid Dynamics Review 2010*, *World Scientific*, 2010, pp. 241-277.

[16] Fluent 6.3 validation guide, Fluent Inc., Lebanon, New Hampshire, USA, 2006.

[17] Cook, P.H., McDonald, M.A., and Firmin, M.C.P., “Aerofoil RAE 2822 - pressure distributions, and boundary layer and wake measurements”, Experimental Data Base for Computer Program Assessment, AGARD Report, AR 138, 1979.

[18] Geissler, W., and Ruiz-Calavera, L.P., “Transition and turbulence modelling for dynamic stall and buffet”, *Engineering Turbulence Modelling and Experiments 4* (Proc. of the 4th Intern. Symposium on Engineering Turbulence Modelling and Measurements), Corsica, France, 1999, pp. 679-688.